

INFLUENCE OF REACTION OPERATION CONDITIONS ON THE FINAL PROPERTIES OF HIGH IMPACT POLYSTYRENE (HIPS)

F. R. Cunha^{1*}, J. M. Costa¹, M. Nele², R. O. M. Folly², M. B. Souza Jr.² and J. C. Pinto³

¹CENPES – Centro de Pesquisas Leopoldo Américo Miguez de Melo, Petrobras,
Phone: + (55) (21) 21624224, Fax: + (55) (21) 21626565, Avenida Horácio Macedo,
Cidade Universitária, Rio de Janeiro, CEP: 21941-915, Rio de Janeiro - RJ, Brazil.

E-mail: frcunha@petrobras.com.br

²Departamento de Engenharia Química, Escola de Química, Universidade Federal do Rio de Janeiro,
Cidade Universitária, CP 68542, CEP: 21949-900, Rio de Janeiro - RJ, Brazil.

³Programa de Engenharia Química/COPPE, Universidade Federal do Rio de Janeiro, Cidade
Universitária, CP 68502, CEP: 21941-972, Rio de Janeiro - RJ, Brazil.

(Submitted: August 11, 2011 ; Revised: August 22, 2012 ; Accepted: August 30, 2012)

Abstract - The main objective of the present work is to analyze the influence of some important operational reaction parameters (agitation speed, polybutadiene – PB – content and initiator concentration) on the final properties of High Impact Polystyrene (HIPS) produced in bulk. Variable effects are analyzed both qualitatively and quantitatively with the help of a fractional factorial design. Physical, chemical and mechanical properties were evaluated through measurement of the weight-average molecular weight (M_w), polydispersity (PD), volume-average diameter of PB particles ($D(4,3)$) and impact strength (Izod). It was found that PD and $D(4,3)$ depend strongly on the initiator concentration, rubber concentration and agitation speed; M_w depends on initiator and rubber concentrations; and Izod depends on the rubber concentration, PD and $D(4,3)$ in the analyzed experimental range. As a consequence, it was shown that control of final polymer properties can be easily performed through proper manipulation of the analyzed operational variables.

Keywords: High Impact Polystyrene; Polymer end-use properties; Experimental design; Modeling; Properties modeling; Impact strength.

INTRODUCTION

High Impact Polystyrene (HIPS) is an important commodity resin because of its improved tenacity (when compared to standard polystyrene), competing with ABS and other impact-resistant plastics in application fields that require good impact properties. Besides, HIPS also presents good optical properties. For this reason, HIPS is used for the manufacture of a large variety of objects, ranging from plastic cups to refrigerator chambers (Albright, 1974).

The main difference between HIPS and General Purpose Polystyrene (GPPS) is the fact that GPPS is constituted of polystyrene molecules, while HIPS is

produced through grafting of polystyrene chains onto previously prepared elastomeric chains (almost always polybutadiene, PB), using suspension or bulk polymerization processes (Choi *et al.*, 2000; Jahanzad *et al.*, 2008). The elastomeric constituent can be dissolved into the initial monomer mixture or added to the reaction media during the polymerization in both suspension and bulk processes. Important quality control properties of HIPS are melt flow index (MFI), deflection temperature under load (DTUL), Vicat hardness, density, Young modulus, strain at break, Rockwell hardness, Izod Impact strength, flexural strength, humidity absorption, mold contraction and flame resistance (Innova

*To whom correspondence should be addressed

product data sheet, 2010). However, the impact resistance usually is the most important end-use property of HIPS for most real applications.

Many papers are devoted to modeling the kinetic aspects of HIPS polymerization (Estenoz *et al.*, 1998; Luciani *et al.*, 2005; Flores-Tlacuahuac *et al.*, 2005^{A,B}), although surprisingly none describes how the final HIPS properties can be related to the reaction conditions and to the characteristics of the final polymer chains. Grassi *et al.* (2001) analyzed the influence of some operational variables on the final properties of HIPS qualitatively. It was shown that the final property values depend on certain operational conditions, although mathematical correlations describing how polymer properties depend on the operational variables and on the characteristics of final polymer chains were not developed.

As a matter of fact, modeling of final polymer properties can be very difficult as they usually depend on the molecular characteristics of the polymer chains produced (such as the molecular weight distribution and composition), on the morphological characteristics of the final material (such as the crystallinity and distribution of crystallite sizes in semi-crystalline materials such as polyethylene and polypropylene) and on the mechanical test conditions (such as dimensions of test samples and test temperatures). Therefore, a suitable description of polymer properties requires detailed modeling of the kinetic mechanism, polymerization reaction and test conditions. For this reason, the use of hybrid modeling approaches can be very useful for most practical purposes. For instance, a useful hybrid model can combine a detailed kinetic model (used to describe the molecular and morphological properties of the obtained polymer material) with an empirical property model (used to describe how end-use polymer properties depend on the molecular and morphological characteristics of the resin and on the analyzed test conditions). Latado *et al.* (2001) and Mattos Neto and Pinto (2001) used similar hybrid approaches to model slurry and bulk propylene polymerizations and were able to describe the final polymer properties (melt flow index, impact resistance, Young modulus and xylene solubles) of commercial polypropylene materials accurately.

The main objective of the present work was to analyze the influence of some important reaction parameters (the agitation speed, the PB content and the initiator concentration) on the final properties of High Impact Polystyrene (HIPS) produced in bulk. Variable effects were analyzed both qualitatively and quantitatively with the help of a fractional factorial design. Physical, chemical and mechanical properties

were evaluated through measurement of weight-average molecular weight (M_w), polydispersity (PD), volume-average diameter of PB particles ($D(4,3)$) and impact strength. It is shown that PD and $D(4,3)$ strongly depend on initiator concentration, rubber concentration and agitation speed. It is also shown that M_w depends on initiator and rubber concentration, while the impact strength depends on the rubber concentration, PD and $D(4,3)$ in the analyzed experimental range. As a consequence, control of final polymer properties can be easily performed through proper manipulation of the analyzed operational variables.

EXPERIMENTAL SECTION

Pre-Polymerization

Reactions were performed in two steps. The first step starts with the solubilization of the PB rubber into styrene. The solution is fed into the reaction vessel with the proper amounts of initiator, chain transfer agent and diluent. Thermal and chemically initiated reactions take place in the first step until monomer conversions reach the range of 30-40 wt%. As the polystyrene content in the reacting media increases, PB domains are formed through precipitation (usually known as phase inversion). In the second step, frequently denoted the devolatilization step and normally performed in a second reaction vessel, the polymerization proceeds until monomer conversions are sufficiently high, usually above 95 wt%. Thermal and chemically initiated reactions also occur in the second reaction step, although the most important chemical reactions in this step are chain crosslinking and grafting of polystyrene chains onto the PB matrix.

Pre-polymerizations were conducted in 1L-reactors (LabMax System, Mettler Toledo, Switzerland), using styrene monomer (polymerization grade, stabilized with tert-butyl catechol) and ethylbenzene (PA) both provided by Innova (Brazil). Tertdodecylmercaptan (TDM) (Innova, Brazil) was used as chain transfer agent and Luperox 331, a bifunctional peroxide from Arkema (USA), was used as initiator. High viscosity (M_w of 340×10^3 Da and Mooney viscosity of 70 at 100 °C) and medium *cis* content (37 mol%) PB was provided by DSM (Netherlands). Chemicals were used as received, without purification.

Agitation speeds, initiator concentrations and PB concentrations were varied in accordance with the proposed experimental design. Reactions were performed at 112 °C for about 150 minutes for the

prepolymerization step. All reactants were initially dissolved in styrene at 80 °C. Samples were collected every 15 minutes for monitoring of monomer conversion with the help of an automatic drying weight balance (Model HR73 Y HG 53, Mettler Toledo, Switzerland).

Devolatilization

Aluminum vessels containing three longitudinal cavities were produced at Petrobras and used as devolatilizers (Figure 1). Each cavity was filled with a closed bottom aluminum liner, containing the previously weighed pre-polymer sample. The vase was closed with an aluminum lid fitted with an orifice for application of vacuum. Heating was applied with an electrical resistance (Dal Pizzol, 2005; Dal Pizzol *et al.*, 2005). Temperature steps between 130 and 250 °C were used in the interval of 250 minutes in a defined profile. Vacuum profiles were imposed on the devolatilizing system when temperature reached 160 °C until complete removal of volatiles, characterized through constant weight determination.

Polymer Characterization

Crosslinked and polystyrene-grafted PB chains form the small gel particles that constitute the elastomeric phase of HIPS. The agitation speed, the PB concentration and the viscosity of the reacting system (which is related mainly to PB molecular

weight before the phase inversion) determine the shape and the size of the dispersed rubber particles. As discussed in the literature, the distribution of rubber particle diameters exerts a pronounced effect on the final HIPS properties (Grassi *et al.*, 2001; Dal Pizzol, 2005). Besides, rubber particles are small and numerous due to more efficient grafting. For this reason, the volume-average diameter of PB particles can also affect the kinetic behavior of the reacting system. Therefore, characterization of particle size is of fundamental importance.

Gel particles were removed from the polystyrene matrix by dissolving the matrix in a solution of toluene and methylethylketone (1.3:1 in volume) and centrifuging the mixture at 20×10^3 rpm (Himac CR 22F, Hitachi, Japan) during 20 min. (Dal Pizzol, 2005; Rovere *et al.*, 2008). Supernatant containing free polystyrene chains was separated and reserved. The precipitated gel was submitted to extraction twice. Gel particles were then coagulated with 30 ml of ethanol. After 30 minutes of resting, gel samples were filtered under vacuum in a sintered melting pot and dried under vacuum at 40 °C for 12 hours. Samples were suspended in methylethylketone (0.0012 g/mL) for size characterization. Gel suspensions were treated in an ultrasound bath for 20 seconds immediately before low angle laser light scattering (LALLS) analyses (Mastersizer Micro Particle Analyzer, Malvern, USA), in order to prevent particle agglomeration. Ethanol was used as the dispersion medium for LALLS characterization, performed at 25 °C.

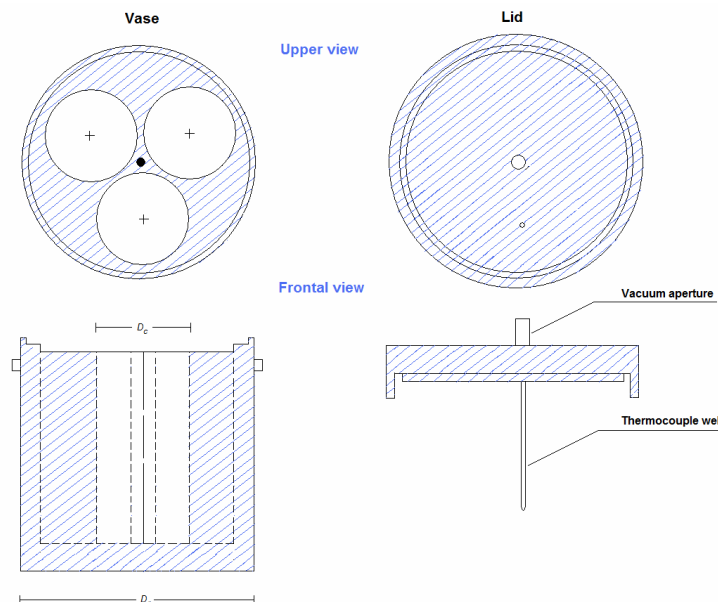


Figure 1: Devolatilizer reactor. D_c – Cavity diameter, D_r – Reactor diameter.

Free polystyrene samples were obtained through centrifugation of the reserved supernatant. Solvent was evaporated under dry nitrogen in a water bath. Dried samples were dissolved in THF (0.15% PS) and used for polymer molecular weight characterization. A gel permeation chromatograph (model 515 HPLC, Waters, USA) equipped with a refractive index detector (model 2410, Waters, USA) was used for characterization of the molar mass distribution. Phenomenogel columns (5 μ m diameter and 300x7.5 mm in length, with porosity ranging from 1.0×10^3 to 1.0×10^6 Å) were used as stationary phases and tetrahydrofuran (THF) was used as solvent. Analyses were performed at 23 °C at 1 ml/min. Calibration was performed with polystyrene standards with M_w values ranging from 9.44×10^3 to 1.24×10^6 Da. Samples were dissolved in THF at 23 °C and filtered in a disposable fluoroprene filter.

Impact strength was measured in a CEAST instrument (Resil Impactor) equipped with a 2J hammer, following ASTM D 256 for Izod impact (ASTM D 256-06a, 2008).^[16] Test pieces were cast in accordance with the ASTM D 4703 molding standard (ASTM D 4703-07, 2007), using an automatic cutter. Before mechanical tests, test pieces were conditioned under controlled atmosphere ($23^\circ\text{C} \pm 2^\circ\text{C}$ and $50\% \pm 5\%$ humidity) for 48 hours.

Experimental Design

Statistica© (version 6.0) was used for data analyses (StatSoft, 2007). A two-level fractional factorial experimental design was proposed to analyze the effects of three distinct operational variables: agitation speed, initiator concentration and PB concentration. It can be expected that modification of the agitation speed and PB content affect the morphology of the elastomeric particles, while modification of the initiator concentration can affect the grafting frequency and the molecular weight distribution of the final resin. As a consequence, the final HIPS properties are expected to change when the analyzed experimental factors are manipulated. A central point

experiment was added to the experimental plan in order to allow the identification of nonlinear effects (Montgomery, 2001). The central point experiment was performed in triplicate in order to characterize the experimental variance (repeatability). Data analyses were always performed with a confidence level of 95%. Experiments were ordered at random. Obtained experimental results are shown in Table 1.

When nonlinear effects were observed to be important, parameter estimation was performed for different model structures. Selected models where the ones that led to the largest correlation between predicted and experimental values and simultaneously allowed for estimation of statistically significant model parameters (confidence level of 95%). Variance analysis was performed in Statistica ©.

RESULTS AND DISCUSSION

Correlation Analysis

Table 2 shows that there are strong and significant linear correlations between the observed M_w , PD and D(4,3) values. This clearly indicates that these variables respond simultaneously to common sources of perturbation. As one can see in Table 2, PD values increase when M_w values decrease. It is important to emphasize that GPC analyses do not provide information about the insoluble gel particles, which means that the homogeneity of the soluble polymer chains increases when the M_w values increase. This probably indicates that part of the rubber can be extracted from the particles when average molecular weights are small, leading to larger PD values. As the M_w values increase, rubber extraction becomes less probable and the homogeneity of the soluble polymer fraction increases. The negative correlation observed between M_w and D(4,3) probably indicates that particle coalescence controls the rubber particle size distribution, as rates of particle coalescence tend to decrease when the viscosity of the reacting medium increases.

Table 1: Experimental design. The higher levels (+) are: initiator concentration, 0.060 wt%; PB concentration, 10 wt%; and agitation speed, 160 rpm. The lower levels (-) are: initiator concentration, 0.030 wt%; PB concentration, 5 wt%; and agitation speed, 80 rpm. Central point (CP) values are the averages in the experimental range.

Experiment	Initiator Concentration	Rubber Concentration	Agitation speed	$M_w 10^3 \text{ g/mol}$	$\frac{M_w}{M_n}$	D(4,3) (μm)	Impact strength (J/m)
1	+	+	+	165	1.99	1.68	75.7
2	+	-	-	196	1.93	2.64	47.5
3	-	+	-	129	3.18	6.76	59.2
4	-	-	+	150	2.70	2.30	31.1
CP1	0	0	0	200	1.88	2.08	54.8
CP2	0	0	0	199	1.81	2.00	58.4
CP3	0	0	0	193	1.80	2.13	64.6

Table 2: Correlation matrix for dependent variables.

	$M_w \times 10^3$ (g/mol)	$\frac{M_w}{M_n}$	$D(4,3)$ (μm)	Impact strength (J/m)
$M_w \times 10^3$ (g/mol)	1	-0.93661	-0.70228	0.11929
$\frac{M_w}{M_n}$	-0.93661	1	0.82470	-0.33571
$D(4,3)$ (μm)	-0.70228	0.82470	1	-0.01617
Impact strength (J/m)	0.11929	-0.33571	-0.01617	1

Statistically significant values are presented in bold.

It is interesting to observe in Table 2 that the impact strength is linearly weakly correlated with the remaining response variables. This probably indicates that the impact strength responds to multiple experimental factors in a more complex manner, justifying the present quantitative study, as discussed below.

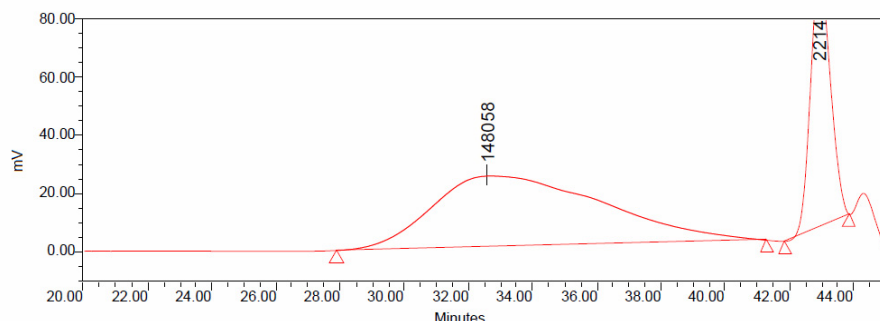
Weight-Average Molecular Weight (M_w)

Figure 2 presents a typical GPC analysis of a HIPS sample. One can see that the molecular weight distributions are very broad and bimodal, indicating that chains of complex molecular structure (linear, grafted and crosslinked chains) may have been extracted from the final polymer samples simultaneously and affected the final GPC results.

Figure 3 presents the Pareto chart for the weight-average molecular weight and shows that the initiator concentration and PB concentration exert the most important effects on M_w . According to Figure 3, the M_w values increase when the initiator concentration increases, while M_w values decrease when the PB concentration increases. Because a bifunctional initiator is used to perform the polymerizations, the

formation of dormant polystyrene chains is possible (Flores-Tlacuahuac *et al.*, 2005^B). Dormant chains can be activated during the devolatilization step, leading to high weight-average molecular weights even when large initiator concentrations are used. In this case, growth of dormant chains in the devolatilization step can explain the increase of M_w with the increase of the initiator concentration. Besides, the increase of the initiator concentration can lead to higher rates of polymer grafting due to reaction of polystyrene radicals with the pendant double bonds, also leading to larger M_w values.

Similarly, when the PB concentration increases, the relative double bond concentration also increases, reducing the relative probability of grafting and crosslinking for individual PB chains. This can explain why the M_w values decrease when the PB concentration increases. Therefore, it seems that chain crosslinking and grafting control the final molecular weight distributions of the obtained polymer samples, as one might already expect. It is also very important to observe that the agitation speed does not affect the M_w values significantly, indicating that this final molecular property of the polymer material do not depend strongly on the morphology of the rubber particles.

**Figure 2:** Typical GPC chromatogram of polymer samples.

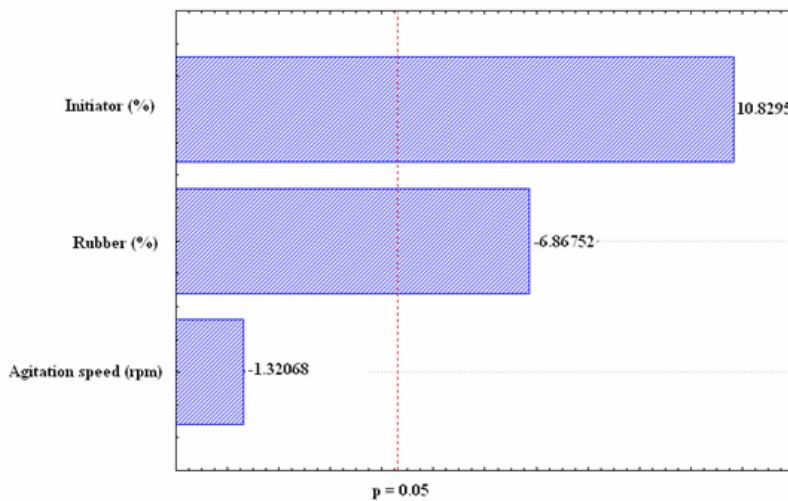


Figure 3: Influence of process variables over M_w .

Figure 4 shows that nonlinear effects cannot be neglected, as the experimental errors cannot explain the differences observed between the experimental and calculated results when only linear terms (main effects) are considered in the analysis. Given the complex kinetic mechanism of the analyzed reaction, one might already expect that nonlinear effects would be significant. For this reason, different empirical nonlinear models were used to represent the obtained data. As the classical free radical polymerization kinetics indicate that M_w is proportional to the inverse of the square root of the initiator concentration (Odian, 2004; Coutinho and Oliveira, 2006), Equation (1) was assumed to be valid, leading to a very good fit of the available experimental data, as also shown in Table 3 and Figure 5.

$$M_w = 1,440.04 - 5.20 \cdot R - 8,469.29 \cdot I - \frac{174.50}{\sqrt{I}} \quad (1)$$

where M_w represents the weight-average molecular weight (in $Dax10^3$), R represents the PB concentration (in wt%) and I represents the initiator composition (in wt%).

Two terms involving initiator concentration can be noted in Equation (1). The first term is related to the conventional monofunctional initiator kinetics, where an increase in initiator concentration corresponds to a decrease of molecular weight. The second term is related to grafting and activation of dormant chain radicals, created by the bifunctional initiator, as an increase of molecular weight averages can be observed with the increase of the initiator concentration.

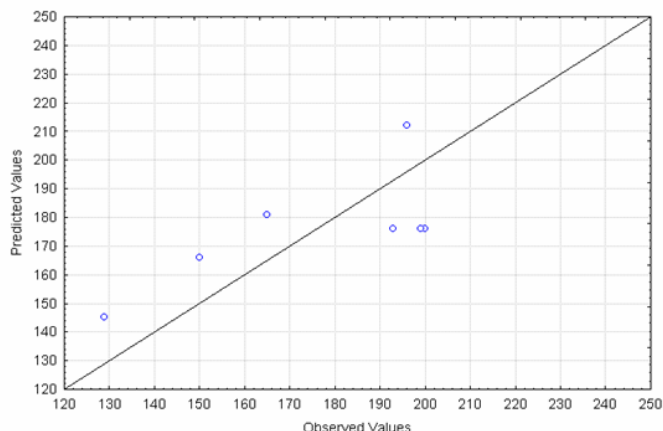
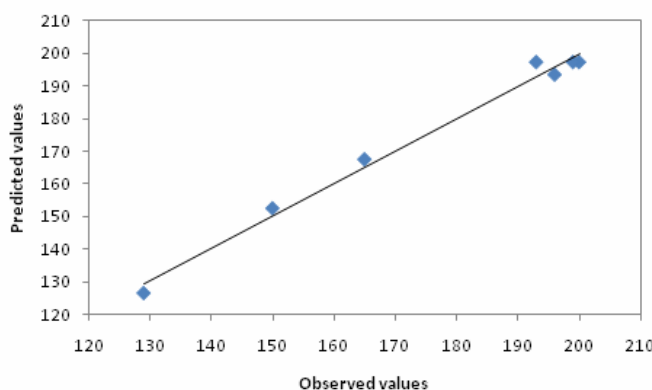


Figure 4: Performance of the linear model for M_w . ($R=0.42$)

Table 3: Estimates for M_w nonlinear model parameters. Although model is non linear in one variable, parameters are linearly estimated.

	Model: $M_w = a + b \cdot R + c \cdot I + \frac{d}{\sqrt{I}}$ Confidence level of 95%						
	Coefficient	Estimate	Standard deviation	t-value	p-level	Lower Limit	Upper Limit
a	1440.04	111.6934		12.8928	0.001007	1084.6	1795.50
b	-5.20	0.8459		-6.1473	0.008660	-7.9	-2.51
c	-8469.29	862.6775		-9.8175	0.002246	-11214.7	-5723.87
d	-174.50	15.0988		-11.5570	0.001391	-222.5	-126.45

**Figure 5:** Performance of the nonlinear model for M_w . ($R=0.99$)

Polydispersity (PD)

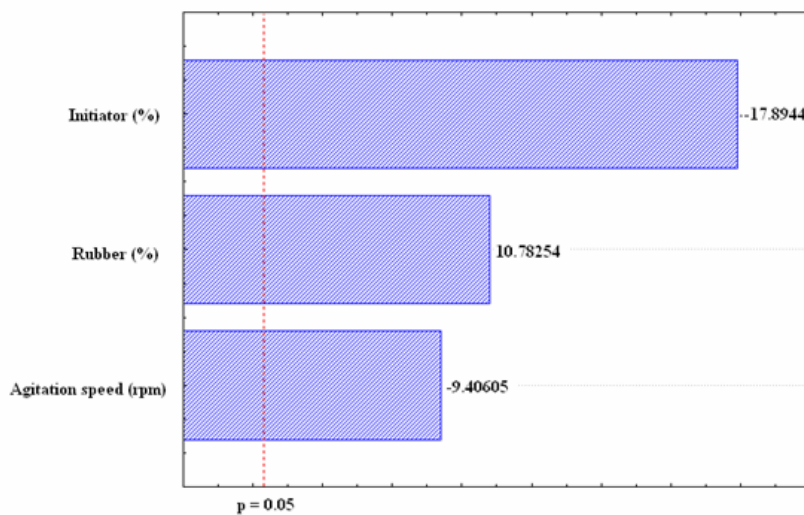
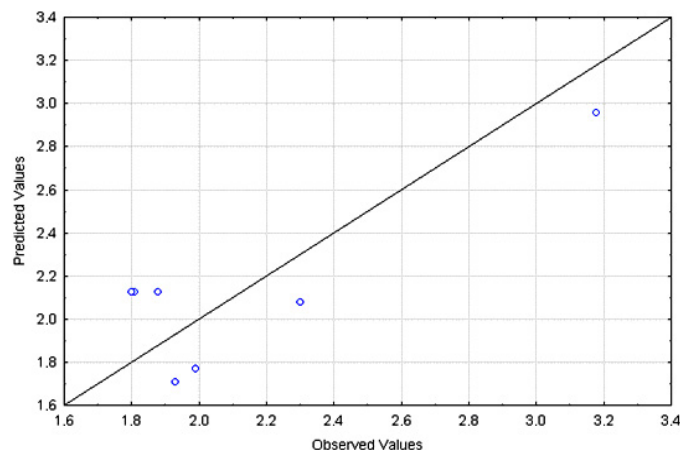
Polydispersity plays an important role in polymer processing, as it is widely accepted that shorter polymer chains can exert a plasticizing effect in the final material and lead to improved processing performance (Odian, 2004). Figure 6 presents the Pareto chart for the polydispersity and shows that all analyzed factors exert significant effects on the PD. The agitation effects are the least important ones, while the initiator concentration effects are the most important ones. According to Figure 6, PD values decrease when the initiator concentration and the agitation speed increase, while PD values increase when the PB concentration increases. Given the strong inverse correlation between M_w and PD values, PD variations can be interpreted as presented in the previous section. The formation of dormant chains leads to higher weight-average molecular weights in the devolatilization step. As shorter chains have greater mobility, grafting and crosslinking take place more efficiently when the initiator concentration in the solution is higher, leading to the simultaneous reduction of the PD. As explained in the previous section, the relative concentration of double bonds increases when the PB concentration increases. This

leads to a reduction of the relative probability of grafting and crosslinking for individual PB chains, increasing the heterogeneity of the polymer chains extracted for GPC analyses.

As performed in the previous case, Figure 7 shows that nonlinear effects cannot be neglected, since the experimental errors cannot explain the differences observed between experimental and calculated results when only linear terms (main effects) are considered in the analysis. As observed previously, one might already expect that nonlinear effects would be significant, given the complex kinetic mechanism of the reaction system. Similarly, different empirical nonlinear models were used to represent the obtained data; however, when Equation (2) was assumed to be valid, a very good fit of the available experimental data was obtained, as shown in Table 4 and Figure 8.

$$\begin{aligned} PD = & -14.7125 + 0.0940 R + 111.0009 I \\ & - 0.0051 Ag + 2.4305 I^{-1/2} \end{aligned} \quad (2)$$

where PD represents the polydispersity, R represents the PB concentration (in wt%), Ag represents the agitation speed (in rpm) and I represents the initiator composition (in wt%).

**Figure 6:** Influence of process variables on PD.**Figure 7:** Performance of the linear model for PD. ($R=0.68$).**Table 4: Estimates for PD nonlinear model parameters. Although model is non linear in one variable, parameters are linearly estimated.**

Coefficient	Model: $PD = a + b \cdot R + c \cdot Ag + d \cdot I + \frac{e}{\sqrt{I}}$ Confidence level of 95%					
	Estimate	Standard deviation	t-value	p-level	Lower Limit	Upper Limit
a	-14.7125	1.152954	-12.7607	0.006085	-19.6733	-9.7518
b	0.0940	0.008718	10.7825	0.008492	0.0565	0.1315
c	-0.0051	0.000545	-9.4060	0.011115	-0.0075	-0.0028
d	111.0009	8.890655	12.4851	0.006354	72.7475	149.2543
e	2.4305	0.155607	15.6195	0.004074	1.7610	3.1000

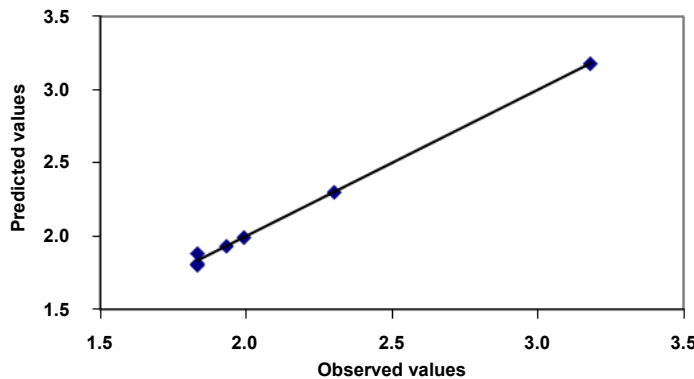


Figure 8: Performance of the nonlinear model for PD. ($R=0.99$).

Particle Diameter (D(4,3))

Figure 9 presents the Pareto chart for D(4,3) and shows that all analyzed factors exert significant effects on D(4,3). In this case, however, the agitation effects are the most important ones, while the kinetic effects are less important. This clearly shows that particle nucleation and coalescence control the volume-average diameters of the final rubber particles. According to Figure 9, D(4,3) values decrease when the agitation speed and the initiator concentration increase, while D(4,3) values increase when the PB concentration increases. The increase of

D(4,3) with increasing PB concentration can be explained in terms of the increasing rubber content, which leads to higher rates of particle nucleation and coalescence. The decrease of D(4,3) values with increasing agitation speeds can be explained in terms of the higher shear rates and, consequently, to the lower rates of particle coalescence. The higher viscosity of reacting media before phase inversion can also lead to higher D(4,3) values. Finally, as the initiator concentration increases, additional grafting takes place, leading to increasing stabilization of occluded PS domains, the amount of the rubbery particle phase and the corresponding D(4,3) values.

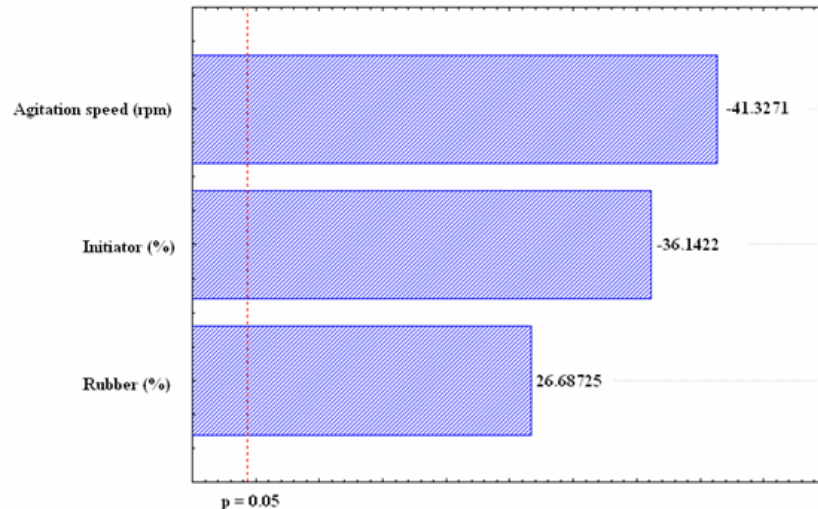


Figure 9: Influence of process variables on D(4,3).

Figure 10 shows once more that nonlinear effects cannot be neglected, as the experimental errors cannot explain the differences observed between experimental and calculated results when only linear terms (main effects) are considered in the analysis. As observed previously, one might already expect that nonlinear effects would be significant, given the complex mechanism that leads to formation of the final rubber particles. Similarly, different empirical nonlinear models were used to represent the obtained data; however, when Equation (3) was assumed to be valid, a very good fit of the available experimental

data was obtained, as shown in Table 5 and Figure 11.

$$\begin{aligned} D(4,3) = & -36.1441 + 0.35 R - 0.0339 Ag \\ & + 256.9156 I + 5.9594 I^{-1/2} \end{aligned} \quad (3)$$

where $D(4,3)$ represents the volume-average diameter of the rubber particles (in microns), R represents the PB concentration (in wt%), Ag represents the agitation speed (in rpm) and I represents the initiator composition (in wt%).

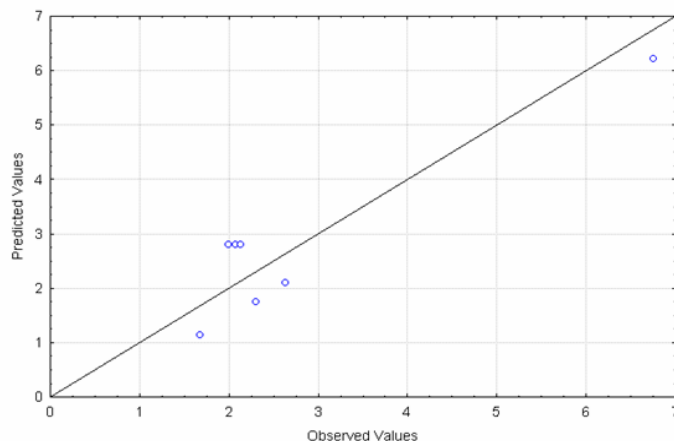


Figure 10: Performance of the linear model for $D(4,3)$. ($R=0.85$).

Table 5: Estimates for $D(4,3)$ nonlinear model parameters. Although model is non linear in one variable, parameters are linearly estimated.

Coefficient	Model: $D(4,3) = a + b \cdot R + c \cdot Ag + d \cdot I + \frac{e}{\sqrt{I}}$					
	Confidence level of 95%					
Coefficient	Estimate	Standard deviation	t-value	p-level	Lower Limit	Upper Limit
a	-36.1441	1.73448	-20.8386	0.002295	-43.6070	-28.6812
b	0.3500	0.01311	26.6872	0.001401	0.2936	0.4064
c	-0.0339	0.00082	-41.3271	0.000585	-0.0374	-0.0303
d	256.9156	13.37492	19.2088	0.002699	199.3680	314.4633
e	5.9594	0.23409	25.4576	0.001539	4.9522	6.9666

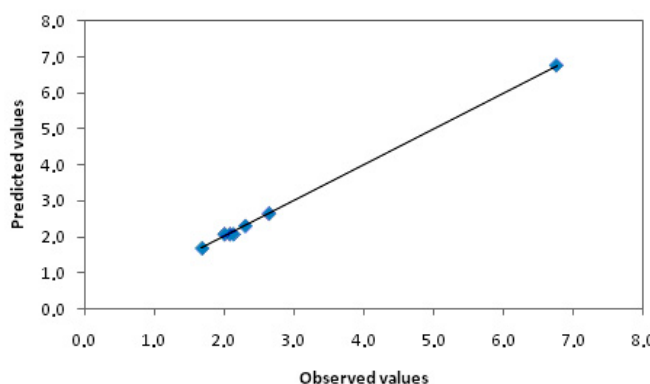


Figure 11: Performance of the nonlinear model for $D(4,3)$. ($R=0.99$)

Impact Strength (Izod)

Figure 12 presents the Pareto chart for the impact strength and shows that only the PB composition affects Izod values significantly. Nevertheless, Latado *et al.* (2001) and León *et al.* (2008) showed that impact resistance can depend on the geometrical properties of the dispersed rubber particles, including the average particle diameters and the interparticle distance, and on the operational variables that lead to modification of the molecular weight distribution of the final polymer material. According to Figure 13, Izod impact cannot be totally explained by

rubber concentration alone. Equation (4) and Figure 14 show that non-linearities involving particle diameter and rubber concentration fit the data very well.

$$\text{Izod} = 123.9992 - 43.5041 \text{PD} + 0.8234D^2 + 0.0036R^4 \quad (4)$$

where Izod represents the impact strength, PD represents free PS polydispersity, R represents PB composition (in wt%) and D represents the volume-average diameter of the rubber particles (in microns).

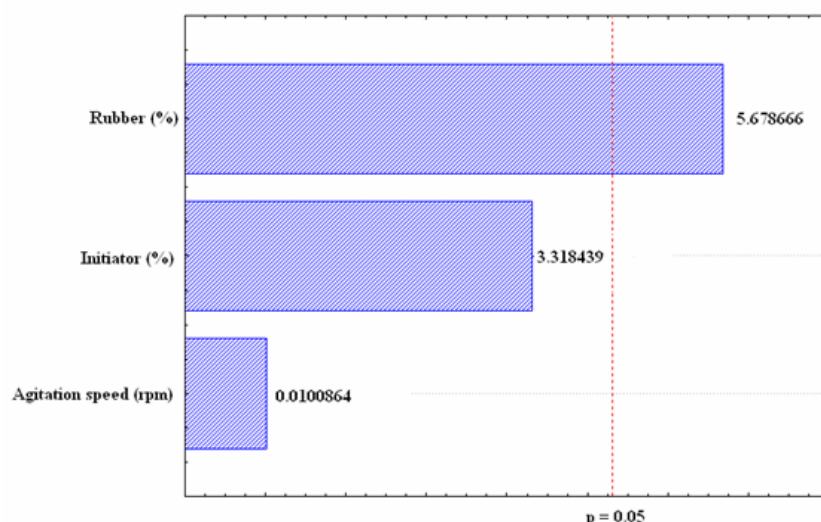


Figure 12: Influence of process variables on Izod.

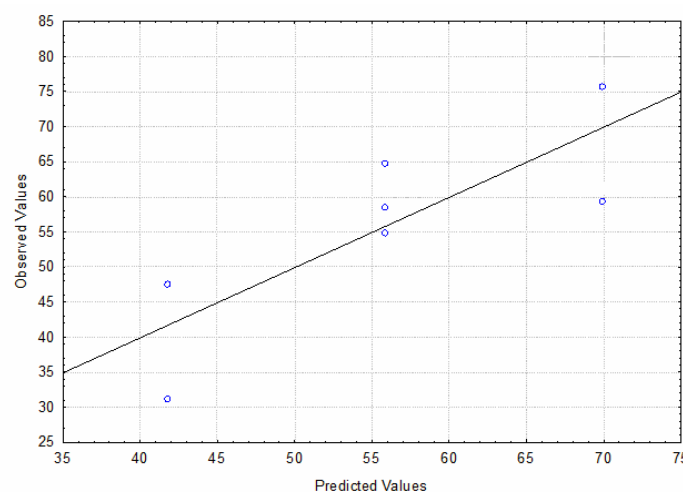


Figure 13: Performance of the linear model for Izod. ($R=0.67$)

Table 6: Estimates for Izod nonlinear model parameters. Although model is non linear in one variable, parameters are linearly estimated.

Coefficient	Model: $Izod = a + b PD + c D^2 + d R^4$ Confidence level of 95%					
	Estimate	Standard deviation	t-value	p-level	Lower Limit	Upper Limit
a	123.9992	12.37093	10.02343	0.002114	84.6293	163.3690
b	-43.5041	6.77241	-6.42373	0.007646	-65.0570	-21.9513
c	0.8234	0.22004	3.74215	0.033295	0.1232	1.5237
d	0.0036	0.00034	10.52831	0.001830	0.0025	0.0047

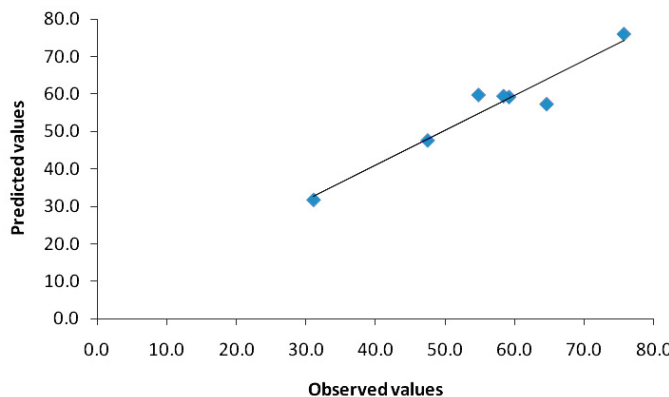


Figure 14: Performance of the non-linear model for Izod ($R=0.93$)

Optimization of Product Performance

Equation (4) indicates that maximization of the impact strength requires maximization of the rubbery phase composition and the average size of the rubber particles and minimization of the free PS polydispersity in the analyzed range. If Equations (2) and (3) are inserted into Equation (4), one concludes that the point of maximum impact strength in the analyzed range is the maximum PB composition, the maximum agitation speed and an intermediary value of the initiator concentration (0.045%), corresponding to operational conditions that are close to conditions of Experiment 1 in Table 1. The maximization of the PB composition leads to maximum average sizes of rubbery particles (Equation (3)), also allowing for maximization of the impact strength (Equation (4)). The minimization of the agitation speed causes an increase of the average particle size, leading to maximization of the impact strength. The existence of an optimum initiator composition that is not located at the boundaries of the analyzed experimental region is due to the square root effect in Equations (1) - (3). According to Equation (4), the maximum attainable impact strength is equal to 81 J/m, which is very similar to the result obtained in Experiment 1 within the experimental error, as

shown in experiments CP1 to CP3. Therefore, it can be assumed that Experiment 1 in Table 1 leads to suboptimum process performance. According to Equations (1) - (4), the optimum operational conditions lead to M_w , PD and $D(4,3)$ values of 184×10^3 Da, 1.86 and 1.58 μm , respectively. Therefore, optimum operational conditions lead to average weight-average molecular weights and very low polydispersity and average particle sizes. These results are comparable to results obtained by Latado *et al.* (2001), who found that the optimum average size of the rubbery phase was close to 0.5 μm in high impact polypropylene materials.

CONCLUSIONS

A fractional factorial experimental design with three factors, two levels and three center points was designed in order to analyze the influence of process variables on high impact polystyrene (HIPS) properties obtained in a bench scale batch process. Initiator concentration, rubber concentration and agitation speed were the independent variables. It was shown that weight-average molecular weight, polydispersity, rubber particle diameter and impact resistance cannot be described as linear functions of the operational variables, due to the complex grafting

and crosslinking reaction steps that take place and control the final product properties. Particularly, it was shown that the point of maximum impact strength in the analyzed experimental range is the maximum PB composition (10 wt%), the maximum agitation speed (160 rpm) and an intermediary value of the initiator concentration (0.045%), which can lead to a final impact strength of 81 J/m.

ACKNOWLEDGMENTS

The authors thank Petrobras for supporting this research. The authors also thank Renível do Nascimento, Raphael Alexandre Albaine Farias da Costa, Marcus Dal Pizzol and Vinicius Grassi for experimental support.

REFERENCES

- Albright, L. F., Processes for Major Addition – Type Plastics and Their Monomers. McGraw-Hill Book Company (1974).
- ASTM D 256-06a, Standard Test Methods for Determining the Izod Pendulum Impact Strength of Plastics (2008).
- ASTM D 4703-07, Standard Practice for Compression Molding Thermoplastic Materials into Test Specimens, Plaques or Sheets (2007).
- Choi, J. H., Ahn, K. H., Kim, S. Y., Effects of the degree of graft on the tensile and dynamic behavior of high impact polystyrene. *Polymer*, 41, p. 5229 (2000).
- Coutinho, F. M. B., Oliveira, C. M. F., Reações de Polimerização em Cadeia – Mecanismos e Cinética. Editora Interciência, Rio de Janeiro (2006). (In Portuguese).
- Dal Pizzol, M. F., Desenvolvimento de poliestireno de alto impacto com balance otimizado de propriedades mecânicas. PhD Thesis, UFRGS, RS (2005). (In Portuguese).
- Dal Pizzol, M. F., Grassi, V. G., Angiolini, F. E., Sandri, G. R., Sistema integrado de polimerização em escala laboratorial e método - PI 0400572-4 (2005). (In Portuguese).
- de León, R. D., Morales, G., Acuña, P., Soriano, F., Mechanical behavior of high impact polystyrene based on SB copolymers as a function of synthesis condition: Part II. *e-Polymers*, no. 15 (2008).
- Estenoz, D. A., Meira, G. R., Gómez, N., Oliva, H. M., Mathematical model of a continuous industrial high impact polystyrene process. *AICHE Journal*, vol. 44, n. 2, p. 427 (1998).
- Flores-Tlacuahuac, A., Saldívar-Guerra, E., Ramírez-Manzanares, G., Grade transition dynamic simulation of HIPS polymerization reactors. *Computers and Chemical Engineering*, 30, p. 357 (2005)^A.
- Flores-Tlacuahuac, A., Zavala-Tejeda, V., Saldívar-Guerra, E., Complex non-linear behavior in the full-scale high-impact polystyrene process. *Ind. Eng. Chem.*, 44, p. 2802 (2005)^B.
- Grassi, V. G., Forte, M. M. C., Dal Pizzol, M. F., Aspectos morfológicos e relação estrutura-propriedades de poliestireno de alto impacto. *Polímeros: Ciência e Tecnologia*, vol. 11, n. 3, p. 158 (2001). (In Portuguese).
- Innova product data sheet at <http://www.petrobras.com.ar/portal/site/PB-eInnova/menuitem.8c1a296aef21c555c0055dd1ed04f0a0/?jsessionid=gT3SLFWQJc90bF4pZS7G42>. (Accessed in January 7, 2010).
- Jahanzad, F., Sajjadi, S., Yianneskis, M., Brooks, B. W., *In-situ* mass-suspension polymerization. *Chemical Engineering Science*, 63, p. 4412 (2008).
- Latado, A., Embiruçu, M., Mattos Neto, A. G., Pinto, J. C., Modeling of end-use properties of poly(propylene/ethylene) resins. *Polymer Testing*, 20, 419 (2001).
- Leal, G. P., Asua, J. M., Evolution of the morphology of HIPS particles. *Polymer*, 50, p. 68 (2009).
- Luciani, C. V., Estenoz, D. A., Meira, G. R., Oliva, H. M., Reduction of transients between steady states in the continuous production of high-impact polystyrene. *Ind. Eng. Chem., Res.*, 44, No. 22, p. 8354 (2005).
- Mattos Neto, A. G., Pinto, J. C., Steady-state modeling of slurry and bulk propylene polymerizations. *Chemical Engineering Science*, 56, p. 4043 (2001).
- Montgomery, D. C., Design and Analysis of Experiments. 5th Edition, John Wiley & Sons (2001).
- Odian, G., Principles of Polymerization. 4th Edition, John Wiley & Sons, Inc., Publication (2004).
- Rovere, J., Correa, C. A., Grassi, V. G., Dal Pizzol, M. F., Caracterização morfológica de poliestireno de alto impacto (HIPS). *Polímeros: Ciência e Tecnologia*, v. 18, n. 1, p. 12 (2008). (In Portuguese).
- StatSoft, Inc. Statistica (Data Analysis Software System), Version 8.0. www.statsoft.com (2007).